NANO LETTERS
Cite This: Nano Lett. 2018, 18, 2864−2869
Letter
pubs.acs.org/NanoLett

Subnanometer Gold Clusters Adhere to Lipid A for Protection against Endotoxin-Induced Sepsis

Fang-Hsuean Liao,[†] Te-Haw Wu,[†] Yu-Ting Huang,[†] Wen-Jye Lin,[‡] Chun-Jen Su,[§] U-Ser Jeng,[§] Shu-Chen Kuo,[∥] and Shu-Yi Lin*[,†]

[†]Institute of Biomedical Engineering and Nanomedicine, National Health Research Institutes, 35053, Taiwan
[‡]Immunology Research Center, National Health Research Institutes, 35053, Taiwan
[§]National Synchrotron Radiation Research Center, 30076, Taiwan
[∥]National Institute of Infectious Diseases and Vaccinology, National Health Research Institutes, 35053, Taiwan

Supporting Information

ABSTRACT: Endotoxicity originating from a dangerous debris (i.e., lipopolysaccharide, LPS) of Gram-negative bacteria is a challenging clinical problem, but no drugs or therapeutic strategies that can successfully address this issue have been identified yet. In this study, we report a subnanometer gold cluster that can efficiently block endotoxin activity to protect against sepsis. The endotoxin blocker consists of a gold nanocluster that serves as a flakelike substrate and a coating of short alkyl motifs that act as an adhesive to dock with LPS by compacting the intramolecular hydrocarbon chain−chain distance (*d*-spacing) of lipid A, an endotoxicity active site that can cause overwhelming cytokine induction resulting in sepsis progression. Direct evidence showed the *d*-spacing values of lipid A to be decreased from 4.19 Å to either 3.85 or 3.54 Å, indicating more dense packing densities in the presence of subnanometer gold clusters. In terms of biological relevance, the concentrations of key pro-inflammatory NF-κB-dependent cytokines, including plasma TNF-α, IL-6, and IL-1β, and CXC chemokines, in LPS-challenged mice showed a noticeable decrease. More importantly, we demonstrated that the treatment of antiendotoxin gold nanoclusters significantly prolonged the survival time in LPS-induced septic mice. The ultrasmall gold nanoclusters could target lipid A of LPS to deactivate endotoxicity by compacting its packing density, which might constitute a potential therapeutic strategy for the early prevention of sepsis caused by Gram-negative bacterial infection.

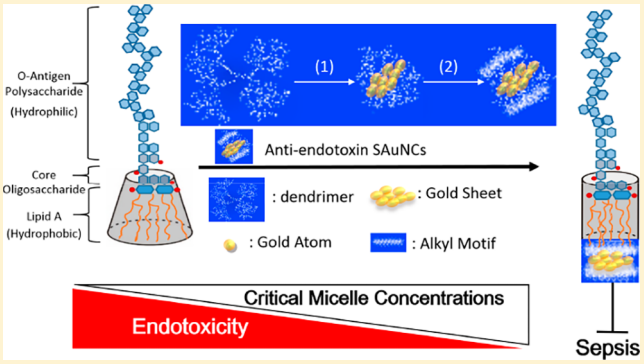

KEYWORDS: *Endotoxin, subnanometer gold clusters, lipopolysaccharide (LPS), lipid A, inflammation, sepsis progression*

Despite endotoxicity constituting a challenging clinical problem, no drugs or therapeutic strategies that can successfully address this issue have been identified yet.[1,2] The dangerous biological outcomes of endotoxicity, including excessive inflammation and even impaired immunity that can potentially lead to fatal sepsis and shock,[1,3] are understood to be strongly associated with the molecular conformation of lipid A of lipopolysaccharide (LPS) due to its influence on the binding affinity of the natural host−guest interaction between the endotoxin (i.e., LPS) and the toll-like receptor 4 (TLR4)-MD2 complex.[4,5] Since LPS is an amphiphilic molecule that can spontaneously self-assemble to form various aggregates under physiological conditions, different aggregate types can change the molecular conformation of lipid A by fine-tuning the intramolecular hydrocarbon chain−chain distance (*d*-spacing) of individual LPS molecules.[6] In general, the conformation of lipid A is simplified for descriptive purposes as consisting of cylindrical and conical shapes, which can be derived from two typical aggregates of LPS, such as lamellar and nonlamellar aggregates.[7] The term "cylindrical and conical shapes" is used because the *d*-spacing distance of individual lipid A domains is either almost equal to or greater than the cross-section of the disaccharide backbone (a portion of an LPS molecule) that acts as a linker to bundle several hydrocarbon chains of lipid A.[4,8] The conformation of lipid A with a conical shape in which the *d*-spacing represents a looser packing density is able to activate the host−guest complex between LPS and the TLR4-MD2 complex for cytokine induction.[9,10] Moreover, the strength profile of cytokine can be dramatically enhanced when the LPS aggregation becomes a cubic type, wherein the lipid A has one of the loosest packing densities. In contrast, the compact packing density between intramolecular hydrocarbon chains seen in lamellar LPS aggregates can result in the reduction or even elimination of cytokine induction.[7,9,11,12] In biological

Received: December 29, 2017
Revised: March 9, 2018
Published: March 28, 2018

Downloaded via SYNCHROTRON RADIATION RESEARCH on January 21, 2019 at 03:49:16 (UTC).
See https://pubs.acs.org/sharingguidelines for options on how to legitimately share published articles.

© 2018 American Chemical Society

DOI: 10.1021/acs.nanolett.7b05464
Nano Lett. 2018, 18, 2864−2869

Scheme 1. A Simple Model Representing the Possible Correlation between the Packing Density of Lipid A of LPS and Sepsis Progression in the Presence of SAuNCs[a]

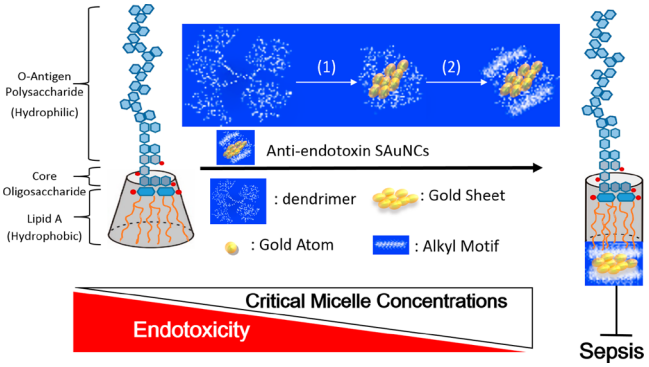

[a]The blue rectangle indicates the formation of a subnanometer gold cluster inside a dendrimer, in which steps 1 and 2 include the synthesis and alkyl-motif modification of gold nanoclusters, respectively, to form antiendotoxin SAuNCs. Please note that the conformation of lipid A is depicted as being conical (left side) and then cylindrical (right side) in shape to correlate with the change of CMC as well as the difference in endotoxicity.

environments, however, the conformation of lipid A is prone to form the looser packing density due to the excellent stability of the cubic aggregate.[13]

In the present work, we sought to construct an ultrasmall gold nanocluster to block endotoxin activity by compacting of the *d*-spacing of lipid A (an endotoxicity active site of LPS). By manipulating the intramolecular packing density, the conformation of lipid A domains can be converted from a looser to a denser density, which could in turn dramatically influence innate immune recognition. The difference in the *d*-spacing resulting in looser or denser packing is a matter of only several angstroms.[14] In order to fine-tune such a subtle change, the antiendotoxin gold nanocluster would need to be composed by an adhesive-like motif consisting of soft materials and an ultrasmall dimension but hard substrate with a flakelike geometry. Such a unique structure would be expected to influence the *d*-spacing of lipid A in addition to increasing the critical micelle concentration (CMC) for the inhibition of LPS nonlamellar aggregation. However, most hard nanometer-scale materials, that is, inorganic nanoparticles, have stereoscopic geometries with different curvatures[15] that make them unsuitable for use as a flakelike substrate. Fortunately, when the size of nanoparticles is shrunk to subnanometer ranges, the geometries of such particles can be changed to flakelike geometries.[16] For example, subnanometer gold clusters (SAuNCs) with a flakelike geometry have already been established theoretically.[17] We hypothesized that such a flattened face of SAuNCs might easily allow an attached adhesive-like motif to dock with the lipid A domain of LPS by compacting the intramolecular *d*-spacing of lipid A (Scheme 1), thereby reducing the recognition of TLR4-MD2 complex for the development of endotoxin-induced sepsis.

Figure 1A shows a blue photoluminescence with excitation and emission peaks at ~390 and ~460 nm, respectively, from the SAuNCs used in this study. While the issue of how to exactly measure the size of SAuNCs poses a big challenge,[18] the

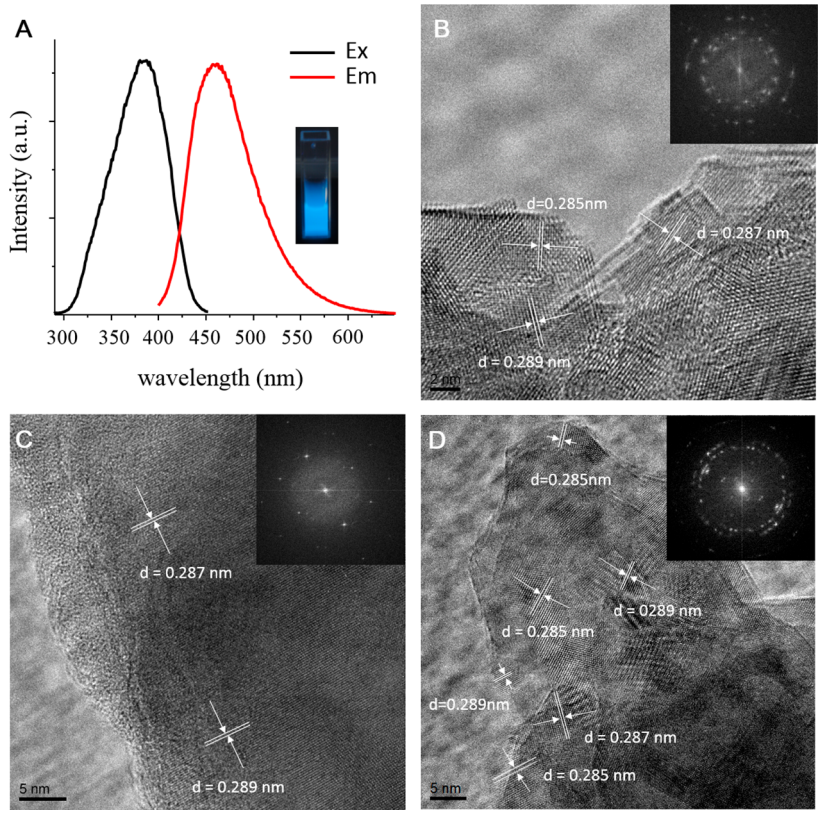

Figure 1. Dimension and stacking of SAuNCs. (A) Photoluminescence spectra and photograph showing the size of the SAuNCs to be less than 1 nm. (B–D) HRTEM images and ED patterns (inset images) of SAuNCs indicating that the gold atoms can self-stack to form thin-films and alignments with different orientations. White arrows show the distances between individual gold atoms.

DOI: 10.1021/acs.nanolett.7b05464
Nano Lett. 2018, 18, 2864–2869

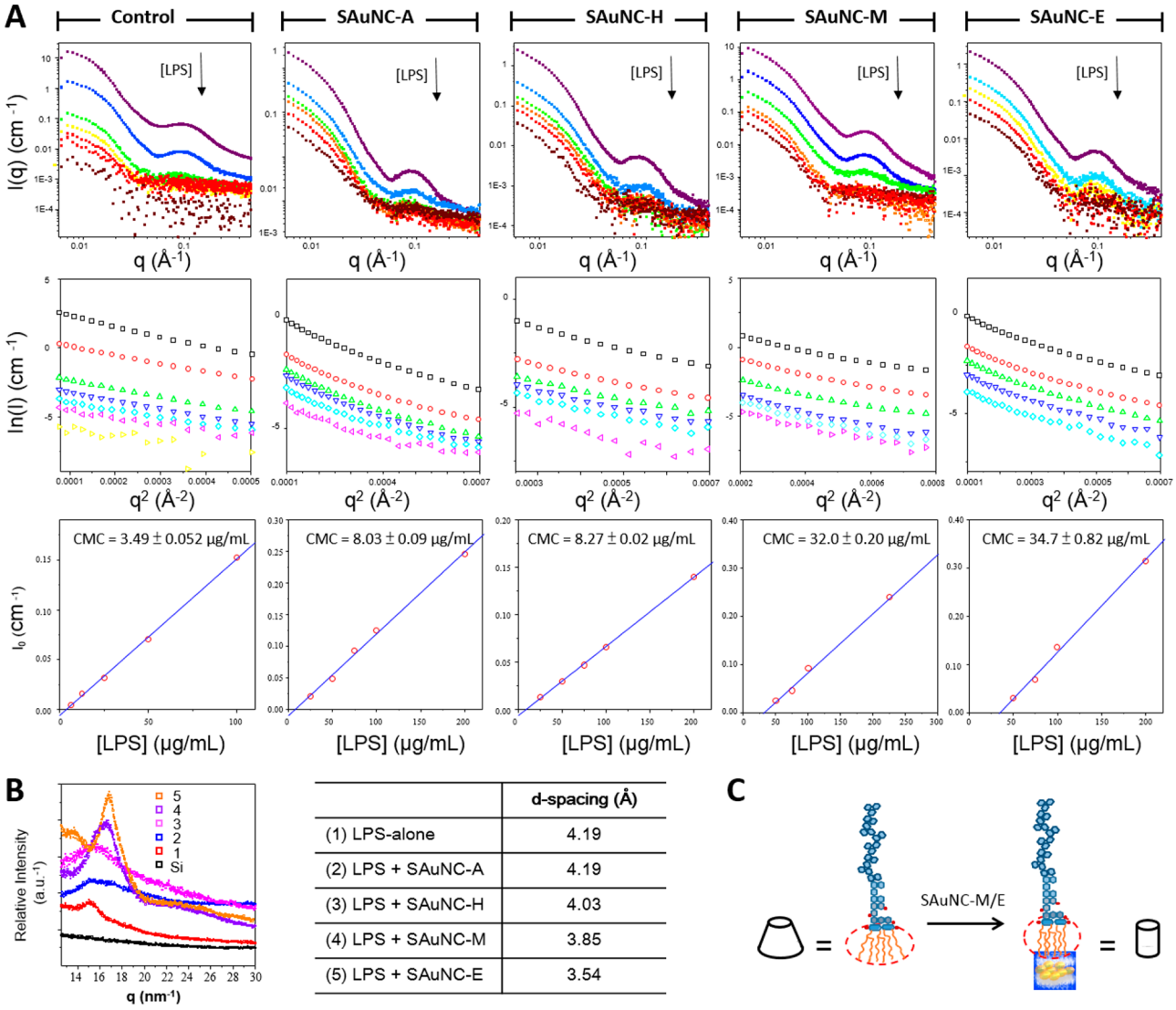

	d-spacing (Å)
(1) LPS-alone	4.19
(2) LPS + SAuNC-A	4.19
(3) LPS + SAuNC-H	4.03
(4) LPS + SAuNC-M	3.85
(5) LPS + SAuNC-E	3.54

Figure 2. Measurement of CMC and *d*-spacing for LPS in the absence and presence of various SAuNCs. The top panels (A) show scattering intensities as a function of q, which are signals from nascent LPS aggregates (micelles or vesicles) at different concentrations in the absence or presence of the four types of SAuNCs. (B) The *d*-spacing measurement of lipid A in the presence of the various SAuNCs. The table summarizes the *d*-spacing distance under each condition. (C) A simple model representing the packing density of lipid A in the presence of either SAuNC-M or SAuNC-E.

emission wavelength of photoluminescence allows for reasonable estimates of how many gold atoms compose a single nanocluster.[19−21] The maximum value of the emission wavelength appearing at ∼460 nm indicates that the SAuNCs are Au_8-dominated nanoclusters (i.e., where Au_8 consists of eight gold atoms).[19,20] The synthetic protocol based on the formation of a dendrimer-encapsulated SAuNCs has been published elsewhere,[19,21] with mass measurements having demonstrated the Au_8-dominated nanocluster within one dendrimer as a main product. Otherwise, the entire size of dendrimer-encapsulated SAuNCs has been reported to be only approximately 2 nm because the embedding of gold atoms can cause an irreversible back-folding of the exterior amines of dendrimers, resulting in the conformation contraction of the dendrimers.[22] It should be emphasized that the conformational contraction of dendrimers can easily happen while adjusting various parameters, including pH and solvent polarity and ion strength.[23,24] The dimension of SAuNCs is estimated to be less than 1 nm and such nanoclusters are thought to possibly have a flakelike shape.[25,26] Thus, we further used a high-resolution transmission electron microscopy (HRTEM) to study the shape of the SAuNCs. It is very surprising that the nanoclusters could form stacks in a layer-by-layer manner (Figure 1B−D) on copper grids, and some domains showed a well-ordered alignment (Figure 1C), from which it can be deduced that these SAuNCs can self-assemble spontaneously into thin-films. Furthermore, we found that the neighbor distance of gold atoms ranged from 0.285−0.289 nm (as indicated by the white arrows shown in Figure 1B−D), which is very close to the theoretical value (i.e., 0.288 nm) of the nearest neighbor spacing.[27] The atomic resolution provides direct evidence to confirm that the alignment was consistent with that of dendrimer-encapsulated SAuNCs rather than gold nanoparticles. That is, the alignment was unlike that of the superstructure of thiol-capped SAuNCs formed from the coalescence of gold atoms, which results in the formation and alignment of gold nanoparticles.[28] The layer-by-layer stacking of the SAuNCs used in this study also illustrated that the

DOI: 10.1021/acs.nanolett.7b05464
Nano Lett. 2018, 18, 2864−2869

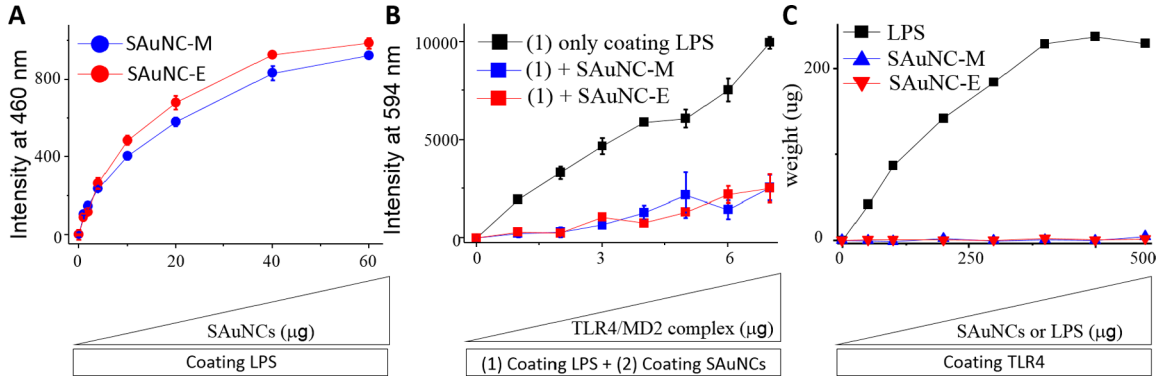

Figure 3. Binding specificity among LPS, SAuNCs and TLR4/MD2 complex. Panel (A) shows the increasing amounts of two kinds of SAuNCs on LPS-coated plates, which was determined by using an ELISA reader to measure the signal of the SAuNCs adsorbed to the plate at an emission wavelength of about 460 nm. Panel (B) shows a noticeable decrease in the binding amount of TLR4/MD2 complex on plates coated with both LPS and SAuNCs in comparison to plates coated with LPS only. The binding specificity of TLR4/MD2 complex was labeled with PE, a dye with an emission wavelength at 594 nm, for measurement. Panel (C) shows no significant interaction between SAuNCs and TLR4. The *y*-axial signal (i.e., amount of LPS-FITC and SAuNCs) was determined by using a calibration curve.

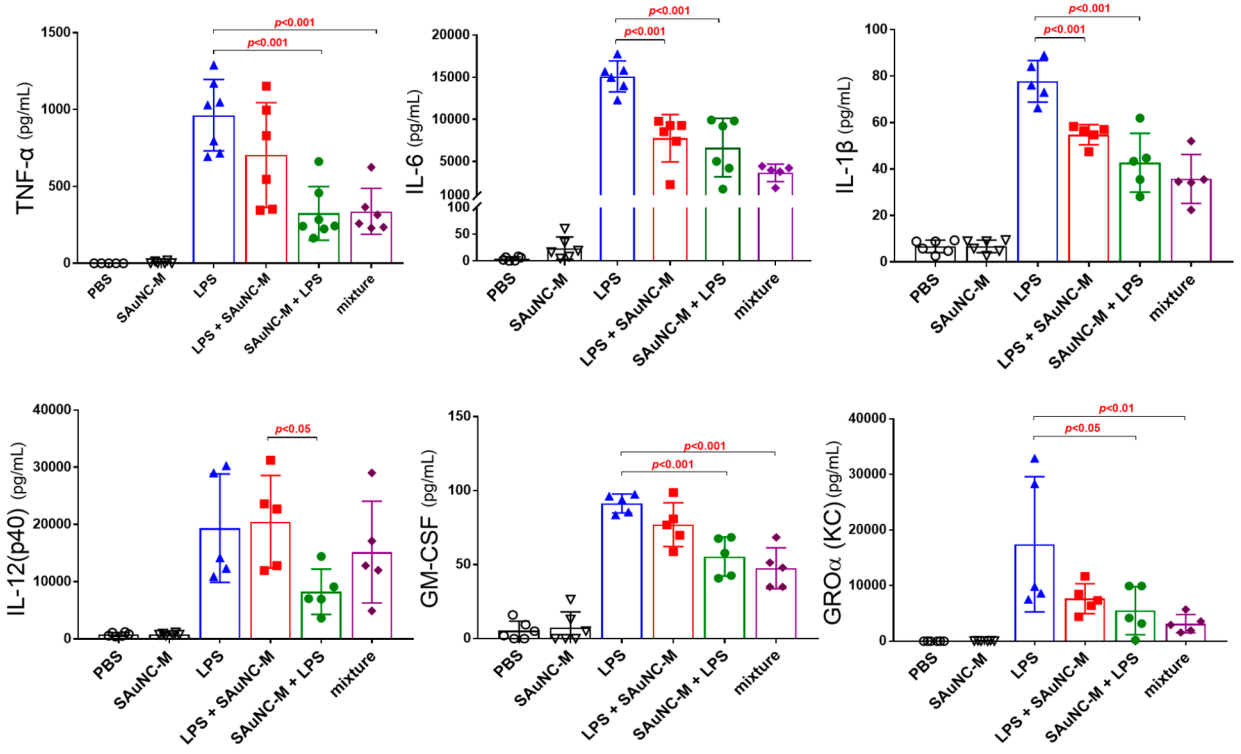

Figure 4. Effect of SAuNC-M on plasma cytokines and CXC chemokines in LPS-challenged mice. Male C57BL/6Narl mice received subcutaneous injections of LPS (0.1 ug) and SAuNC-M (7.5 ug) into the hind footpad at the indicated time points. Blood samples were harvested at 1 and 2 h after the second treatment for the measurement of TNF-α and other cytokines, respectively.

capping molecule (i.e., the deformed dendrimer) might avoid the coalescence of gold atoms, as well as assist in the self-assembly of the SAuNCs. As a result, the observation of thin-films also can explain that the geometry of SAuNCs consists of a flakelike structure that can allow layer-by-layer alignment. On the basis of this observation, the SAuNCs were then decorated with two kinds of alkyl motifs, methyl and ethyl groups, that were used as adhesives and resulted in the SAuNC-M and SAuNC-E, respectively. The detailed synthesis and characterization of these SAuNCs are described in the Supporting Information and shown in Figures S1 and S2.

Next, it is very interesting to determine whether the CMC of LPS can be influenced in the presence of either SAuNC-M or SAuNC-E, resulting in the inhibition of LPS aggregation. For comparison, we also prepared other hydrophilic and hydrophobic SAuNCs (denoted as SAuNC-A and SAuNC-H, respectively) that did not, however, include the decorative alkyl-motifs that have been validated to cause LPS aggregates;[29] that is, the CMC of the LPS could not be affected by them. Figure 2A (the top row) shows an intense signal around 0.1 A^{-1} that determined the aggregate formation of LPS in the absence and presence of various SAuNCs by small-angle X-ray scattering (SAXS). According to Guinier analysis,[30] the forward scattering intensity (I_0) was obtained by fitting a linear plot of $\ln(I)$ as a function of the square of the measured scattering intensity (q^2) (Figure 2A, the middle row). Because the I_0

DOI: 10.1021/acs.nanolett.7b05464
Nano Lett. 2018, 18, 2864−2869

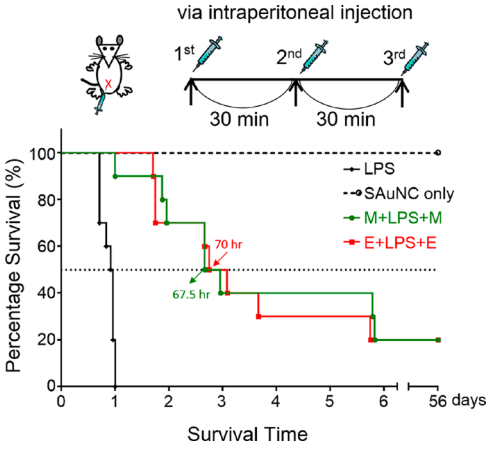

Figure 5. Survival rates of mice with LPS-induced sepsis (25 mg/kg BW) subjected to the treatments with the two kinds of SAuNCs (75 mg/kg BW). The dash line represented the half percentage survival. M and E indicate the SAuNC-M and SAuNC-E, respectively.

showed a good linearity in relation to the low solution concentrations (Figure 2A, the bottom row), the CMC values of the LPS in each condition could then be calculated via linear extrapolation. As expected, Figure 2A (the fourth/fifth column) shows that the CMC value of the LPS in the presence of either SAuNC-M or SAuNC-E was significantly increased (by a 10-fold magnitude) over that of the LPS alone (the first column). These effects might be attributed to the interactions of the methyl and ethyl motifs on the SAuNCs with lipid A, which could have resulted in the inhibition of the self-assembly process of LPS. Thus, the measurement of the *d*-spacing of lipid A by using grazing-incidence wide-angle X-ray scattering (GIWAXS) was shown in Figure 2B (the left side). The results found that both SAuNC-M and SAuNC-E caused an observable change of scattering vector ($\mathbf{q}$), changing it from 14.96 to 16.32 and 17.72 nm^{-1}, respectively. The values of the *d*-spacing ($2\pi/\mathbf{q}$) for lipid A in each condition were then calculated, and listed in Figure 2B (the right side). The *d*-spacing values are about in distribution from 4.19 to 3.54 Å. It is notable that only SAuNC-H/M/E resulted in compacting of the *d*-spacing of lipid A in comparison to the *d*-spacing for lipid A seen with LPS alone; that is, SAuNC-A resulted in no compacting. These results indicated that SAuNCs with hydrophobic moieties, especially those with only methyl and ethyl motifs, could reduce the intramolecular *d*-spacing of each individual LPS molecule, resulting in more dense packing densities from lipid A (Figure 2C), in addition to increasing the CMC of LPS, and that might be protecting against sepsis.

Besides the SAuNCs that can directly dock the lipid A of LPS, as mentioned above, it is required to evaluate whether SAuNC-M and SAuNC-E can or cannot act as an antagonist to bind with TLR4/MD2 complex as well. As expected, we found that both SAuNC-M and SAuNC-E can bind to LPS and present a dose-dependent response (Figure 3A), but cannot associate with TLR4 (Figure 3C). As a result, the conclusion that our SAuNCs behaved as TLR4 antagonists can be ruled out. More importantly, the association of LPS and the TLR4/MD2 complex is dramatically reduced in the presence of SAuNC-M and SAuNC-E in comparison to their association in the presence of LPS alone (Figure 3B). This observation suggested that SAuNC-M and SAuNC-E might only engage with the lipid A of LPS to interrupt the interactions between LPS and various proteins. As such, based on our strategy the SAuNCs might become an effective inhibitor for antiendotoxin.

The hypothesis that the compacting of lipid A by the SAuNCs can protect mice from LPS-induced inflammation needs to be validated. Note that neither SAuNC-M nor SAuNC-E alone is regarded as an immune stimulant (Figure S3). For simplification, only SAuNC-M was investigated by a detailed study of the induction of key pro-inflammatory cytokines and chemokines in LPS-challenged mice. Regardless of the pretreatment or post-treatment of SAuNC-M injections, the inhibition of LPS-induced cytokine/chemokine induction was comparable to the injections of the premix of LPS and SAuNC-M (Figures 4 and S4, purple column, labeled as mixture). For example, the concentrations of pro-inflammatory NF-κB-dependent cytokines, including plasma TNF-α, IL-6, and IL-1β in the LPS-challenged mice were significantly reduced. Again, the plasma immunostimulatory IL-12p70 levels were not changed, whereas the plasma IL-12p40 levels resulting from pretreatment with SAuNC-M were lower than those resulting from post-treatment with SAuNC-M. IL-12p40 plays an immunoregulatory role as the bridge between innate and adaptive defense immunity.[31] Meanwhile, the levels of both plasma GM-CSF and GROα (KC), which are secreted by innate immune cells in response to LPS challenge,[1] were significantly decreased in the mice that underwent SAuNC-M injection. Other production of plasma cytokines and CXC chemokines profiles (Figure S4) as well as expression of phosphorylated NF-κB (Figure S5) from RAW264.7 and bone marrow-derived macrophage (BMDM) also showed a noticeable decrease. Taken together, the results suggest that the SAuNCs might affect lipid A function and thereby lead to a decrease in the cell cytotoxicity of endotoxin during earlier events after LPS injection.

Pharmacokinetics study shows that the 17.4 h half-life of SAuNC-M was slightly longer than that of SAuNC-E (15.4 h) (Table S1). The preventive effect in LPS-induced septic mice of using SAuNC-M and SAuNC-E was validated (Figure 5). Because our SAuNCs could not kill Gram-negative bacteria (Table S2), the experimental sepsis mimicked the release of endotoxin debris after bacterial death.[32] While the median survival time of LPS-induced septic mice without SAuNC injections was 22.5 h, the median survival time of LPS-induced septic mice pretreated with SAuNC-M and SAuNC-E was 67.5 and 70 h, respectively. Two kinds of SAuNCs (i.e., SAuNC-M and SAuNC-E) significantly prolonged the survival time with a three-fold increase in LPS-induced septic mice. The survival time of the LPS-induced septic mice injected with SAuNC-E was slightly longer than that of the LPS-induced septic mice injected with SAuNC-M. It is speculated that this greater improvement was because the ethyl motifs could adhere more strongly to lipid A than the methyl motifs due to an intermolecular van der Waals force. Collectively, the SAuNCs with decorated methyl and ethyl motifs might potentially function as an endotoxin blocker.

In summary, we present herein a subnanometer gold cluster that can efficiently block endotoxin activity as a means of counteracting sepsis. The endotoxin blocker consists of a gold nanocluster that serves as a flakelike substrate and a coating of short alkyl motifs that act as an adhesive for docking with LPS, a dangerous debris of Gram-negative bacteria, through targeting lipid A and compacting its intramolecular hydrocarbon chain−chain distance (*d*-spacing). In biological relevance, the induction of key pro-inflammatory NF-κB-dependent cyto-

DOI: 10.1021/acs.nanolett.7b05464
Nano Lett. 2018, 18, 2864−2869

kines, including plasma tumor necrosis factor-alpha (TNF-α), IL-6 and IL-1β and chemokines in LPS-challenged mice showed a noticeable decrease. Not only that the treatment of antiendotoxin SAuNCs could significantly prolong the survival time in LPS-induced septic mice. The injection of antiendotoxin SAuNCs might constitute a potential therapeutic strategy for the early prevention of sepsis caused by Gram-negative bacterial infection, effectively protecting the patients from systemic inflammatory response syndrome (SIRS), septic shock, and sepsis-induced lethality.

■ ASSOCIATED CONTENT

Supporting Information

The Supporting Information is available free of charge on the ACS Publications website at DOI: 10.1021/acs.nanolett.7b05464.

Materials and methods and other associated figures, tables, and references (PDF)

■ AUTHOR INFORMATION

Corresponding Author

*E-mail: shuyi@nhri.org.tw.

ORCID

Wen-Jye Lin: 0000-0001-8821-9813

U-Ser Jeng: 0000-0002-2247-5061

Shu-Yi Lin: 0000-0002-6871-6617

Notes

The authors declare no competing financial interest.

■ ACKNOWLEDGMENTS

We thank the National Health Research Institutes of Taiwan (NHRI-BN-105/106-PP-30) and the Ministry of Science and Technology of Taiwan (MOST-106-2113-M-400-005) for providing financial support for this research. Special thanks go to Dr. Y. W. Su (Immunology Research Center, National Health Research Institutes, Taiwan), Dr. C. P. Liu (Department of Chemistry, Fu Jen Catholic University, Taiwan), Dr. T. K. Yeh (Institute of Biotechnology and Pharmaceutical Research, Taiwan), and Mr. C. N. Yao and Miss S. P. Chen for their advice regarding the choice of mice gender, TEM measurements, the data analysis of the pharmacokinetics study, and the western blot analysis, respectively.

■ ABBREVIATIONS

NF-κB, nuclear factor kappa B; TNF-α, tumor necrosis factor-alpha; IL, interleukin; GM-CSF, granulocyte macrophage colony-stimulating factor; GROα/KC, growth-related oncogene-alpha/keratinocyte-derived chemokine; RANTES, regulated and normal T cell expressed and secreted; MIP-1α, macrophage inflammatory protein-1α; G-CSF, granulocyte-colony stimulating factor; CCL2−5, CC chemokine ligand 2−5

■ REFERENCES

(1) Hotchkiss, R. S.; Sherwood, E. R. *Science* **2015**, *347*, 1201−1202.

(2) Perner, A.; Rhodes, A.; Venkatesh, B.; Angus, D. C.; Martin-Loeches, I.; Preiser, J. C.; Vincent, J. L.; Marshall, J.; Reinhart, K.; Joannidis, M.; Opal, S. M. *Intensive Care Med.* **2017**, *43*, 496−508.

(3) Hotchkiss, R. S.; Moldawer, L. L.; Opal, S. M.; Reinhart, K.; Turnbull, I. R.; Vincent, J. L. *Nat. Rev. Dis. Prim.* **2016**, *2*, 16045.

(4) Xiaoyuan Wang, P. J. Q. *Endotoxins: Structure, Function and Recognition*; Springer: Dordrecht, 2010; Vol. *53*.

(5) Park, B. S.; Lee, J. O. *Exp. Mol. Med.* **2013**, *45*, e66.

(6) Brandenburg, K.; Funari, S. S.; Koch, M. H. J.; Seydel, U. *J. Struct. Biol.* **1999**, *128*, 175−186.

(7) Seydel, U.; Oikawa, M.; Fukase, K.; Kusumoto, S.; Brandenburg, K. *Eur. J. Biochem.* **2000**, *267*, 3032−3039.

(8) Moran, A. P.; Brennan, P. J.; von Itzstein, M. *Microbial Glycobiology: Strucutres, Relevance and Applications*; Elsevier Inc., 2009.

(9) Brandenburg, K.; Mayer, H.; Koch, M. H. J.; Weckesser, J.; Rietschel, E. T.; Seydel, U. *Eur. J. Biochem.* **1993**, *218*, 555−563.

(10) Seydel, U.; Hawkins, L.; Schromm, A. B.; Heine, H.; Scheel, O.; Koch, M. H. J.; Brandenburg, K. *Eur. J. Immunol.* **2003**, *33*, 1586−1592.

(11) Brandenburg, K.; Seydel, U.; Schromm, A. B.; Loppnow, H.; Koch, M. H. J.; Rietschel, E. T. *J. Endotoxin Res.* **1996**, *3*, 173−178.

(12) Netea, M. G.; van Deuren, M.; Kullberg, B. J.; Cavaillon, J. M.; Van der Meer, J. W. M. *Trends Immunol.* **2002**, *23*, 135−139.

(13) Brandenburg, K.; Koch, M. H. J.; Seydel, U. *J. Struct. Biol.* **1990**, *105*, 11−21.

(14) Kastowsky, M.; Sabisch, A.; Gutberlet, T.; Bradaczek, H. *Eur. J. Biochem.* **1991**, *197*, 707−716.

(15) Jin, R. C.; Zeng, C. J.; Zhou, M.; Chen, Y. X. *Chem. Rev.* **2016**, *116*, 10346−10413.

(16) Hakkinen, H. *Chem. Soc. Rev.* **2008**, *37*, 1847−1859.

(17) Han, Y. K. *J. Chem. Phys.* **2006**, *124*, 024316.

(18) Azubel, M.; Koivisto, J.; Malola, S.; Bushnell, D.; Hura, G. L.; Koh, A. L.; Tsunoyama, H.; Tsukuda, T.; Pettersson, M.; Hakkinen, H.; Kornberg, R. D. *Science* **2014**, *345*, 909−912.

(19) Zheng, J.; Petty, J. T.; Dickson, R. M. *J. Am. Chem. Soc.* **2003**, *125*, 7780−7781.

(20) Zheng, J.; Zhang, C. W.; Dickson, R. M. *Phys. Rev. Lett.* **2004**, *93*, 077402.

(21) Jao, Y. C.; Chen, M. K.; Lin, S. Y. *Chem. Commun.* **2010**, *46*, 2626−2628.

(22) Chien, C. T.; Liu, C. Y.; Wu, Z. W.; Chen, P. J.; Chu, C. L.; Lin, S. Y. *J. Mater. Chem. B* **2014**, *2*, 6730−6737.

(23) Welch, P.; Muthukumar, M. *Macromolecules* **1998**, *31*, 5892−5897.

(24) Boas, U.; Christensen, J. B.; Heegaard, P. M. H. *J. Mater. Chem.* **2006**, *16*, 3785−3798.

(25) Furche, F.; Ahlrichs, R.; Weis, P.; Jacob, C.; Gilb, S.; Bierweiler, T.; Kappes, M. M. *J. Chem. Phys.* **2002**, *117*, 6982−6990.

(26) Gilb, S.; Weis, P.; Furche, F.; Ahlrichs, R.; Kappes, M. M. *J. Chem. Phys.* **2002**, *116*, 4094−4101.

(27) Laibinis, P. E.; Whitesides, G. M.; Allara, D. L.; Tao, Y. T.; Parikh, A. N.; Nuzzo, R. G. *J. Am. Chem. Soc.* **1991**, *113*, 7152−7167.

(28) Santiago-Gonzalez, B.; Monguzzi, A.; Azpiroz, J. M.; Prato, M.; Erratico, S.; Campione, M.; Lorenzi, R.; Pedrini, J.; Santambrogio, C.; Torrente, Y.; De Angelis, F.; Meinardi, F.; Brovelli, S. *Science* **2016**, *353*, 571−575.

(29) Luo, Y. H.; Wu, Z. W.; Tsai, H. T.; Lin, S. Y.; Lin, P. P. *Nano Lett.* **2015**, *15*, 6446−6453.

(30) Glatter, O.; Kratky, O. *Small angle X-ray scattering*; Academic Press: London, 1982.

(31) Abdi, K. *Scand. J. Immunol.* **2002**, *56*, 1−11.

(32) Nemzek, J. A.; Hugunin, K. M.; Opp, M. R. *Comp. Med.* **2008**, *58*, 120−128.

DOI: 10.1021/acs.nanolett.7b05464
Nano Lett. 2018, 18, 2864−2869